

Epoxy–Diamine Thermoset/Thermoplastic Blends. 1. Rates of Reactions before and after Phase Separation

A. Bonnet, J. P. Pascault,* H. Sautereau, and M. Taha

Laboratoire des Matériaux Macromoléculaires-UMR CNRS 5627, Institut National des Sciences Appliquées, 20, Avenue A. Einstein, 69621 Villeurbanne Cedex, France

Y. Camberlin

Institut Français du Pétrole-Industrial Research and Development Center BP 3, 69390 Vernaison, France

Received November 12, 1998; Revised Manuscript Received May 17, 1999

ABSTRACT: Rates of epoxy–amine reactions in thermoset/thermoplastic blends with different thermoplastic concentrations were studied. The selected thermoset system was bisphenol A diglycidyl ether cured with 4,4'-methylenebis[3-chloro-2,6-diethylaniline] in the presence of various concentrations of polyetherimide (PEI) (10–64 wt %). As the initial systems are homogeneous, the rate constants for the epoxy–amine neat system and the rate constants of the blends are the same, the addition of PEI in the epoxy–amine system leads only to a dilution of reactive groups during this first step. But due to the epoxy–amine reaction, a liquid–liquid phase separation occurs at a given conversion (in the range 0.2–0.4). At the same time and for PEI concentrations equal or higher than 30 wt %, a sudden increase of the reaction rate is observed from experimental results. Comparison between blends based on PEI and polystyrene (PS) shows that after phase separation the reaction rate of the PS blend was higher than the PEI blend due to a faster phase separation process for the PS blend. Estimations of the new dilution ratio of the two phases have been made through glass transition temperature measurements. Modeling of the kinetics of the epoxy–amine reaction in each phase of a 48 wt % PEI blend have been made. The increase of the reaction rate at phase separation can be explained by the formation of an epoxy–amine-rich phase with a faster reaction rate. Modeling permits to predict that gelation in this phase occurs at a conversion close to 0.6.

Introduction

Thermoset (TS)/thermoplastic (TP) blends are materials resulting from the mixing of the TP polymer with the TS precursor (generally a diepoxy–diamine system) and the subsequent reaction of this precursor. Usually the initial mixture is homogeneous, and due to the molar mass increase of the TS precursor, a liquid–liquid phase separation occurs at a given conversion.¹ The beginning of the phase separation process can be determined by light transmission (LT), light scattering (LS), or small-angle X-ray scattering (SAXS). Depending on the technique used, the observation scales can be different.

One important factor controlling the phase separation process and the morphologies generated is the location of the composition of the initial blend, ϕ_{TP}^0 , with respect to the critical composition, $\phi_{TP,crit}$. For a TP with average molar masses between 10 000 and 30 000 g/mol, $\phi_{TP,crit}$ in diepoxy–diamine TS precursors may be obtained from the Flory–Huggins model and is in the range 10–15 wt % TP.¹ In a previous study, Girard-Reydet et al.² demonstrated that for quantities of TP, ϕ_{TP}^0 in the range of $\phi_{TP,crit}$ (10 wt % for example), phase separation during epoxy–amine reaction proceeded by spinodal demixing (SD) and LT or LS gave a correct estimation of the beginning of the phase separation process. For off-critical compositions (typically ≥ 30 wt %), the second phase appeared through nucleation and growth (NG). In this case SAXS was able to observe the beginning of the phenomena before LT or LS. It was also shown that

for $TP \leq 10$ wt % the continuous phase was the epoxy–amine network, and for $TP \geq 30$ wt % the continuous phase was the TP. However, the 10–30 wt % formed an ill-defined bicontinuous morphology.

These morphological differences are studied for two reasons: (i) modification of TS networks with high-performance ductile TP³ ($TP \leq 15\%$) or (ii) new processing routes for intractable high-temperature-resistant TP polymers,^{4–5} ($TP \geq 30\%$).

Most of the studies on TS–TP blends were mainly focused on final morphologies and/or mechanical properties.^{1–3, 6} However, to control the morphologies and properties requires a good knowledge of the different events occurring during the reaction of the TS precursor. For this reason the aim of this work is to investigate the effects of the TP concentration on TS chemistry (part 1) and on the rheological behavior of the blend (part 2).

The thermoplastics used were two nonfunctionalized thermoplastics: polyetherimide, PEI, and polystyrene, PS. The TS precursor is composed of a diglycidyl ether of bisphenol A, DGEBA, and an aromatic diamine as curing agent, 4,4'-methylenebis(3-chloro-2,6-diethylaniline), MCDEA. Both mixtures before any reaction exhibit an upper critical solution temperature (UCST) with $T_{max} \approx 50$ °C for PEI⁷ and $T_{max} \approx 125$ °C for PS. This means that PS was less soluble than PEI in the TS precursor. At curing temperature higher than 130 °C both types of TP are soluble. Furthermore, the liquid–liquid phase separation will arrive earlier for PS than for PEI during isothermal cure.

The mechanism and kinetics of the epoxy/amine curing reactions have been widely analyzed; three principal reactions take place:

* To whom correspondence should be addressed.

Table 1. Characteristics of the Blend Components

Reactant	Formula	Supplier
4,4'-methylene-bis[3-chloro-2,6-diethylaniline] MCDEA $M = 380 \text{ g.mol}^{-1}$		Lonza
diglycidyl ether of bisphenol A DGEBA $\bar{n}=0.15$ $M_n = 382.6 \text{ g.mol}^{-1}$		Ciba Geigy LY556
Polyetherimide PEI $M_n = 26000 \text{ g.mol}^{-1}$ $M_w = 50000 \text{ g.mol}^{-1}$ $T_g = 210^\circ\text{C}$		General Electric Ultem 1000
Polystyrene PS $M_n = 90000 \text{ g.mol}^{-1}$ $M_w = 246000 \text{ g.mol}^{-1}$ $T_g = 99^\circ\text{C}$		ATO Chem Lacquirene 1070N

the ratio of eqs 6 and 7) and a_1 and a_2 (integrating the ratio of eqs 7 and 8) are found, chemical kinetics for a stoichiometric system may be expressed by¹³

$$\frac{dx}{dt} = (1-x)[K'_1 + K_1 F(\alpha)][2(1-r)\alpha + r\alpha^{n/2} + (2-r)F(\alpha)L]/(2-r) \quad (10)$$

$$\frac{d\alpha}{dt} = -2\alpha(1-x)[K'_1 + K_1 F(\alpha)] \quad (11)$$

$$F(\alpha) = 1 + \frac{(\text{OH})_0}{e_0} - [(1-r)\alpha + \alpha^{n/2}]/(2-r) \quad (12)$$

The chemical rate constants k_1 , K'_1 , and k_3 with an Arrhenius temperature dependence were determined for the DGEBA $\bar{n} = 0.03$ /MCDEA system in a previous work.⁸ In the present work the liquid DGEBA ($\bar{n} = 0.15$) was used; the initial $[\text{OH}]_0/e_0$ ratio is equal to 0.075.

If the addition of a TP in the epoxy–amine system leads only to a dilution of reactive functions, the rate constants for the epoxy neat system ($k_{i,N}$) and the rate constants of the blend ($k_{i,B}$) must be the same, which leads to

$$K_{1,B} = K_{1,N} \frac{e_{0,B}^2}{e_{0,N}^2} \quad \text{and} \quad K'_{1,B} = K'_{1,N} \frac{e_{0,B}}{e_{0,N}} \quad (13)$$

The ratio $e_{0,B}/e_{0,N}$ can be expressed as a function of ω = mass fraction of TP, ρ_N = density of the epoxy–amine

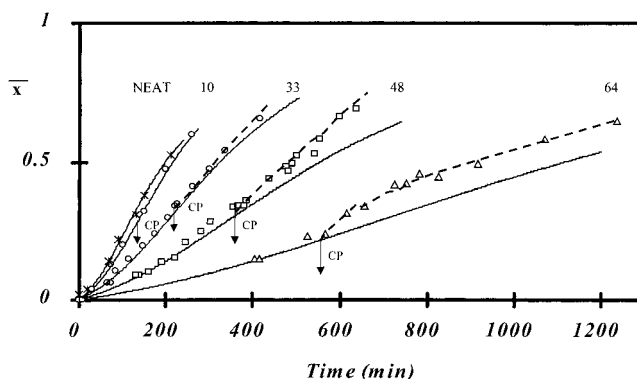


Figure 2. Influence of the PEI concentration on the epoxy–amine DGEBA ($\bar{n} = 0.15$)–MCDEA reaction. Curing is done at 135°C . Epoxy conversion is measured by HPLC. The full lines indicate modeling by using the experimental results from ref 8 (see text for details). Points are experimental results (mean value, \bar{x} , after phase separation). Arrows indicate the cloud points, determined by light transmission.

copolymer, and ρ_{TP} = density of the thermoplastic, TP:

$$\frac{e_{0,B}}{e_{0,N}} = \left(1 + \frac{\omega}{1-\omega} \frac{\rho_N}{\rho_{TP}}\right)^{-1} \quad (14)$$

Different kinetic measurements have been made at the same curing temperature $T_i = 135^\circ\text{C}$. In Figure 2 are reported different results:

(i) The experimental results for the neat system, DGEBA ($\bar{n} = 0.15$)–MCDEA (experimental points in Figure 2) and its kinetic modeling (line in Figure 2): The values of the chemical rate constants used for the modeling are the ones from ref 8, considering that some

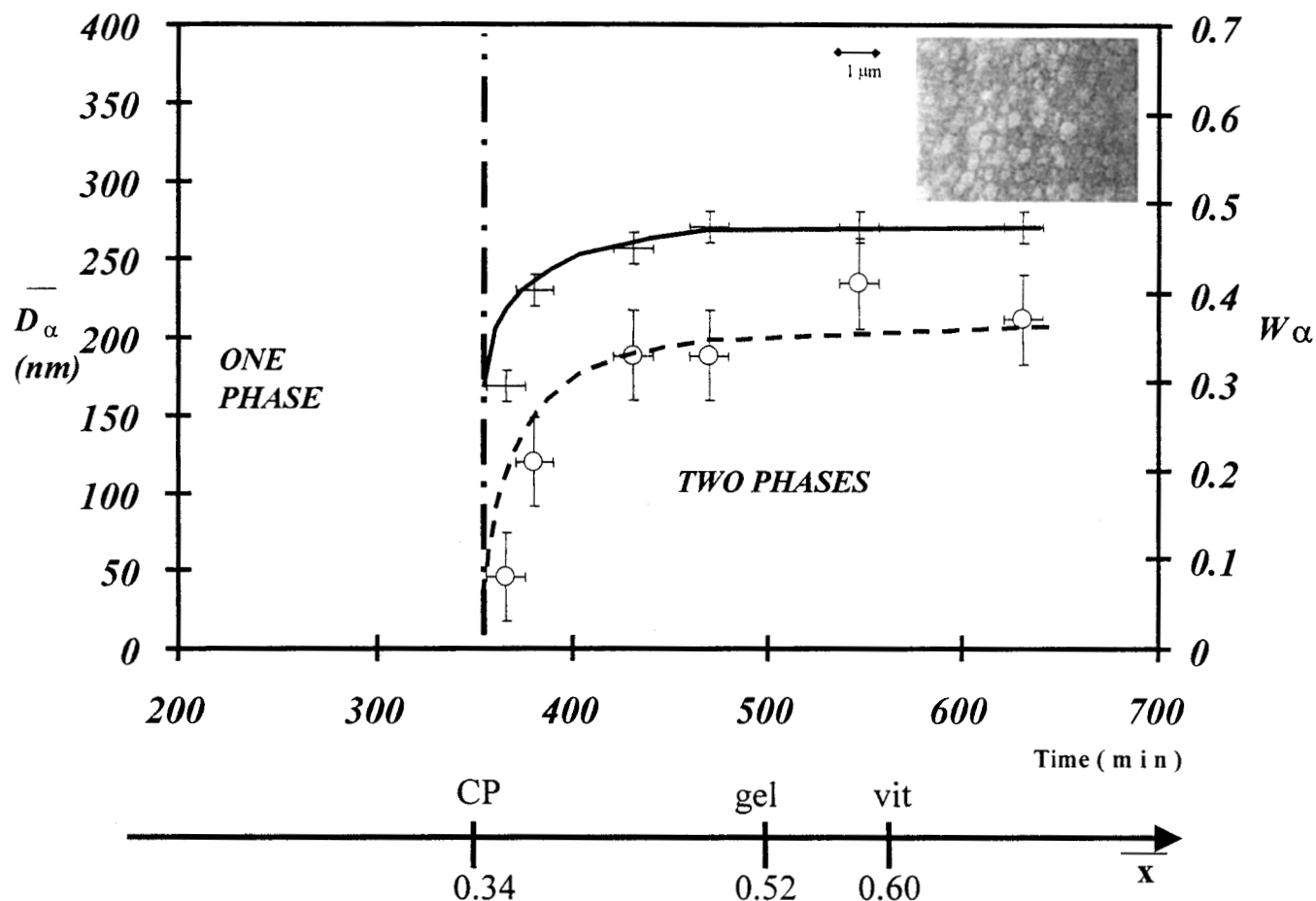


Figure 3. Evolutions of the mean diameter, \bar{D} , of the dispersed particles observed by TEM (—) and their estimated concentration, W_α (---), during the reaction of a 48 wt % PEI/DGEBA ($\bar{n} = 0.15$)—MCDEA blend cured at $T_i = 135^\circ\text{C}$. The photo represents the final morphology at the end of the curing stage at 135°C (TEM).

etherification reactions are possible and taking into account our initial $[\text{OH}]_0/e_0$ ratio (use of eqs 10–12).

(ii) The kinetic predictions for four blends with four different PEI concentrations, $\phi_{\text{TP}}^0 = 10, 33, 48$, and 64 wt % TP (four lines in Figure 2): The kinetic predictions take into account the kinetic model for the neat system and a dilution effect induced by the presence of the thermoplastic (use of eqs 13 and 14).

(iii) The experimental results obtained for the four blends (experimental points in Figure 2): For 10 wt % PEI the mixing of the different reactants was simple, and the initial reaction time, t_0 , at 135°C was easily obtained. But for samples prepared with the twin-screw extruder, during mixing some epoxy–amine reactions occurred. Therefore, at the beginning of the kinetic measurements at 135°C an initial $x > 0$ exists: 0.06 for 33 PEI, 0.09 for 48 PEI, and 0.15 for 64 PEI. To solve this problem, we have assumed that the first experimental points obtained follow the kinetic model. (This can also be reasonably assumed and will be confirmed later with PS as the thermoplastic.)

(iv) And finally, the cloud point (CP) times determined by light transmission (indicated by arrows) represent the beginnings of the phase separation process: The CPs have been observed by the LT technique, even though we know that for $\text{PEI} \geq 30$ wt % the beginning of phase separation observed by SAXS is before. For example, for 30 wt % PEI, $x_{\text{CP}} = 0.35$ but $x_{\text{SAXS}} = 0.15$. This has been explained by the fact that for these TP quantities the mechanism of phase separation is nucle-

ation and growth instead of spinodal demixing for 10–20 wt %.²

For blends the developed kinetic model in homogeneous medium can be applied only before phase separation. From Figure 2 it appears that for all thermoplastic concentrations, throughout the one-phase region (before phase separation in the range of CP arrows), the addition of PEI leads to a dilution of epoxy–amine functions. Even if the extent of reaction with time decreases with PEI content, the real kinetic rate constants are not modified in the one-phase area.

Upon phase separation, dispersed particles are formed which grow in size and number. Morphologies can be observed by TEM at different levels of the phase separation process. Figure 3 gives an example of the two-phase structure which was observed in the case of the blend 48 wt % PEI at the end of curing step at 135°C . Figure 3 illustrates also the evolution of the mean diameter, \bar{D} , and the estimated concentration of the dispersed phase, W_α (in this case, the epoxy–amine-rich phase). As after phase separation two phases coexist with unknown epoxy–amine concentrations in each phase, the kinetic model developed for homogeneous medium cannot be applied after phase separation. During phase separation the dilution ratios change rapidly and differently in the epoxy-rich (α) phase and the thermoplastic-rich (β) phase. These dilution ratios are also changing with reaction times. The experimental epoxy conversion which is measured after phase separation is an overall measurement of conversions in both

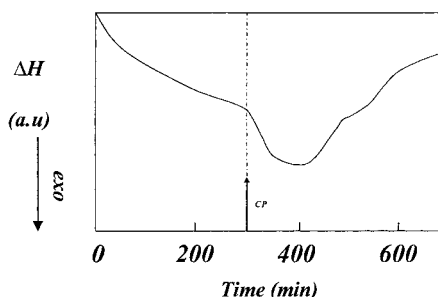


Figure 4. DSC scan at $T_i = 135\text{ }^{\circ}\text{C}$ for the DGEBA($\bar{n} = 0.15$)–MCDEA/48 wt % PEI blend.

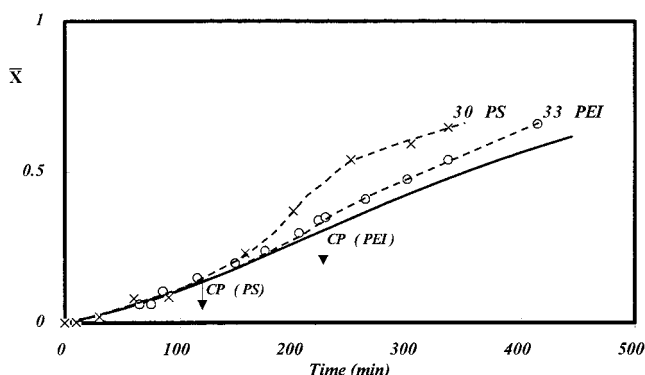


Figure 5. Influence of the type of TP on the epoxy–amine reaction of the DGEBA($\bar{n} = 0.15$)–MCDEA system. $T_i = 135\text{ }^{\circ}\text{C}$, experimental points for PS (+) and PEI (o), (mean \bar{x} , value after phase separation). The full line indicates the modeling (cf. Figure 2).

phases. The mean conversion of epoxy groups will be noted \bar{x} .

Looking back to Figure 2, it can be said that for low TP concentration, (e.g., 10 wt %) and confirming our previous results,¹⁹ the kinetic fit is rather good during all of the reaction. This means that after phase separation the experimental points are not precise enough to see a difference with the predictions from the initial dilution effect (due to the low concentration of the TP-rich β phase (the dispersed phase in this case)). But when the TP concentrations are high enough to have a TP continuous phase ($\phi \geq 30$ wt % PEI),⁷ the fitting between the prediction from the initial dilution effect and the experimental points is only observed up to the time where the phase separation process begins (experimentally between CP measured by SAXS and LT). After this point a sudden increase of reaction rate is observed.

For PEI > 30 wt %, the value of $\Delta\bar{x}$ between the kinetic model and the experimental mean values becomes more and more important as the weight percent PEI increases. This effect can also be observed when the ΔH of the reaction is measured by DSC (Figure 4). For this reason (but also for other reasons as vitrification of β phase, etc.) classical isothermal DSC experiments are very difficult to quantify. It would be necessary to use modulated DSC.²⁰

Comparison between two Thermoplastics, PS and PEI. To be sure that this effect of the phase separation phenomena on the reaction rate can be generalized to different blends, a comparative experiment has been done with another nonfunctionalized TP. Figure 5 gives the comparison between the model and the experimental evolutions of epoxy conversion for DGEBA($\bar{n} = 0.15$)–MCDEA reactions with 30 wt % PS

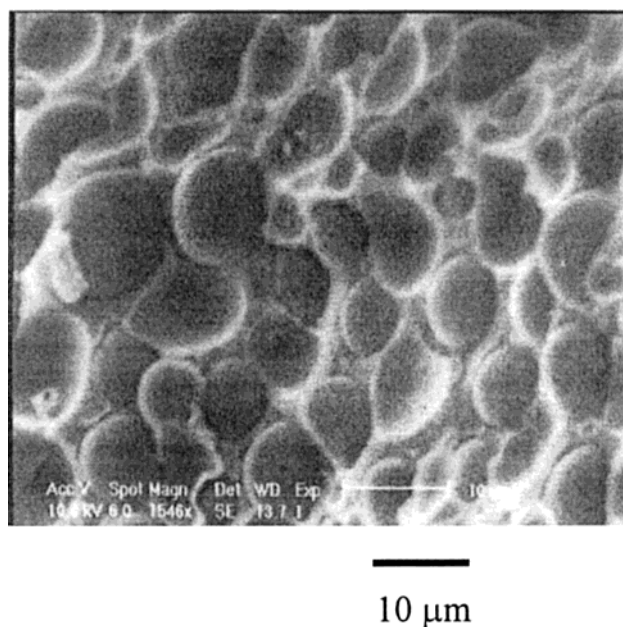


Figure 6. Photo of the final morphology of 30 wt % PS blend (SEM) (cured 5 h at $135\text{ }^{\circ}\text{C}$ and postcured for 2 h at $185\text{ }^{\circ}\text{C}$).

and 33 wt % PEI. One advantage of this experiment with PS was that the blending was easier and faster in this case than with PEI (due to the lower T_g of PS). Furthermore, the initial conversion at the end of the twin-screw extruder process was zero, which means that we had the possibility to obtain many kinetic experimental points before the CP.

The kinetic effect was confirmed. Before phase separation the experimental points were predicted by the kinetic model, taking into account only the initial dilution effect, and was independent of the nature of the nonfunctionalized TP. Alternatively, an increase of the reaction rate was observed when the phase separation had occurred. This kinetic increase was greater for PS than for PEI. Explanations for this difference between PS and PEI are twofold:

(i) PS is less soluble than PEI. Therefore, phase separation occurs at a lower conversion x , which means a less viscous system and a faster transfer of monomers and i -mers between β and α phases than in the case of PEI. This leads to a higher average particle size (comparison between Figures 3 and 6).

(ii) At $T_i = 135\text{ }^{\circ}\text{C}$ the TP-rich β phase vitrifies in the case of PEI but not in the case of PS. This means that with the PS system mass transfers from β to α phases are possible up to the end of the reaction.

Modeling of the Rate of the Epoxy–Amine Reaction after Phase Separation in α and β Phases.

As stated earlier, upon phase separation the dilution ratio changed rapidly and differently for α and β phases. These new two dilution ratios were also changing with reaction times. The epoxy conversion, which was measured by liquid chromatography (HPLC), was the average epoxy conversion of the epoxy conversions in α and β phases. Equation 5 was used to calculate x from the disappearance of epoxy monomer, \bar{X} ; eq 5 was now expressed by two terms:

$$1 - \bar{X} = (1 - x_\alpha)^2 \phi_\alpha + (1 - x_\beta)^2 \phi_\beta \quad (15)$$

where ϕ_α and ϕ_β are the mass fractions of epoxy in α and β phases.

To know these x_α and x_β values, it would be necessary to know the concentration of the disperse phase and the compositions of α and β phases at each time. In the absence of direct measurements, an idea for a rough estimation was to use glass transition temperature, T_g , measurements. Using the Couchman equation,²¹ and by considering that each phase is homogeneous, it is possible to write for the α and β phases

$$\ln T_{g(\alpha)} = \frac{M_{1(\alpha)}\Delta C_{p1(\alpha)} \ln T_{g1(\alpha)} + [1 - M_{1(\alpha)}]\Delta C_{p2} \ln T_{g2}}{M_{1(\alpha)}\Delta C_{p1(\alpha)} + [1 - M_{1(\alpha)}]\Delta C_{p2}} \quad (16)$$

$$\ln T_{g(\beta)} = \frac{M_{1(\beta)}\Delta C_{p1(\beta)} \ln T_{g1(\beta)} + [1 - M_{1(\beta)}]\Delta C_{p2} \ln T_{g2}}{M_{1(\beta)}\Delta C_{p1(\beta)} + [1 - M_{1(\beta)}]\Delta C_{p2}} \quad (17)$$

where subscript 1 indicates the epoxy-amine reactive solvent, subscript 2 indicates the thermoplastic, M_i is the weight ratio of i in the mixture, and T_{gi} and ΔC_{pi} are the glass transition temperature and the heat capacity change at T_g of component i . T_g (ΔC_p) of component 1 (epoxy-amine) is changing with conversion \bar{x} , while T_g (ΔC_p) of component 2 (TP) is constant.

Two other equations taking into account the mass conservation can be written:

$$\frac{\Delta C_{p(\alpha)}}{W_\alpha} = M_{1(\alpha)}\Delta C_{p1(\bar{x})} + [1 - M_{1(\alpha)}]\Delta C_{p2} \quad (18)$$

$$\frac{\Delta C_{p(\beta)}}{W_\beta} = M_{1(\beta)}\Delta C_{p1(\bar{x})} + [1 - M_{1(\beta)}]\Delta C_{p2} \quad (19)$$

in which W_α is the weight fraction of α and W_β of β phase.

Before any calculation, it was necessary to have T_g (ΔC_p) measurements. Figure 7 gives T_g (ΔC_p) values obtained for the 48 wt % PEI blend which was expected to have the best precision. When the mixture was homogeneous, one T_g is observed. However, after the CP, two T_g 's were observed, with one higher and one lower than the T_g of the previous homogeneous phase. The upper one, $T_{g(\beta)}$, was attributed to the PEI-rich phase while the lower one, $T_{g(\alpha)}$, was attributed to the epoxy-amine-rich phase. Both had different evolutions with curing time.

$T_{g(\beta)}$ increased because of the rise of the thermoplastic concentration in the β phase (the continuous phase), until it reached the curing temperature $T_i = 135^\circ\text{C}$. At that time vitrification of the β phase occurred, $t_{\text{vit}(\beta)} = 550$ min (Figure 7a), and mass transfers from β to α ceased.

Changes of the T_g of the dispersed phase, $T_{g(\alpha)}$, were more complex. Roughly two main processes can be assumed: (i) epoxy-amine monomers or dimers were transferred from the β to the α phase and (ii) epoxy-amine reactions occurred in the α phase. Between t_{cp} and $t_i = 450$ min, $T_{g(\alpha)}$ was practically constant, due to the arrival in the α phase of new monomers, dimers, etc., from the β phase. At $t_i \geq 450$ min $T_{g(\alpha)}$ increased rapidly due primarily to the increase of the molar mass of the epoxy-amine i -mers. The gelation time of the α phase, which was the time at which an insoluble fraction appeared, was measured at $t_{\text{gel}} = 500$ min in the area of $T_{g(\alpha)}$ increase. This fast increase of $T_{g(\alpha)}$ was observed

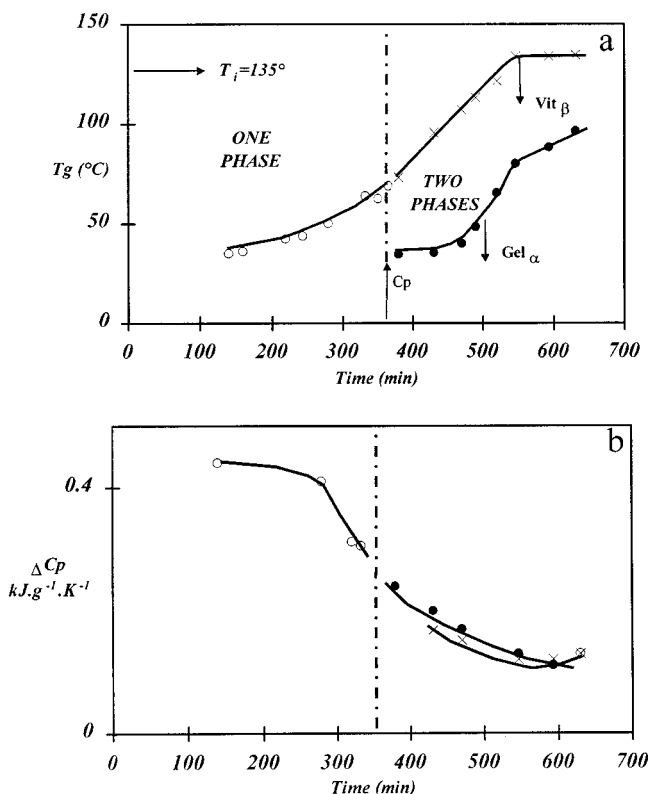


Figure 7. T_g (a) and ΔC_p (b) evolutions during the reaction of the PEI 48 wt %/DGEBA ($\bar{n} = 0.15$)–MCDEA blend cured at $T_i = 135^\circ\text{C}$: (○) homogeneous phase, (●) α phase, (×) β phase.

Table 2. Compositions of Each Phase as a Function of Mean Conversion \bar{x} ^a

$\bar{x} \pm 0.035$	$M_{1,\alpha} \pm 0.1$	$M_{1,\beta} \pm 0.1$	$W_\alpha \pm 0.05$	$W_\beta \pm 0.05$	$W_\alpha + W_\beta \pm 0.1$
0.36	0.85	0.48	0.35	0.63	0.98
0.44	0.9	0.44	0.35	0.65	1
0.48	0.9	0.37	0.42	0.54	0.96

^a $M_{1,\alpha,\beta}$ = mass fraction of epoxy-amine i -mers in both phases. $W_{\alpha,\beta}$ = mass fraction of both phases.

up to $t_i = 540$ min, which was in the same range as the vitrification of the β phase. After this point the rate of increase of $T_{g(\alpha)}$ lessened due to a decrease of the reaction rate. This can be explained by a decrease of the epoxy-amine concentration due to reactions and the absence of transfer between β and α phases.

By comparing Figures 3 and 7a, it is clear that the final diameter of dispersed particles was reached before the vitrification of the β phase detected by DSC. Vitrification is not a well-defined transition, and rheological measurements at different frequencies showed that vitrification of β phase started earlier, in the same range as the particle's growth stopped (part 2²³). This means that the morphology of the dispersed phase was controlled by different parameters including the vitrification of the continuous phase. It was also shown that this effect was not totally deleted by a postcure.²⁻⁶

The evolutions of ΔC_p with t_i (Figure 7b) are very complex and will not be discussed.

Coming back to the first aim of this part, estimations of epoxy conversion in α , (x_α) and β (x_β) phases could be done from T_g (ΔC_p) measurements by using eqs 16–19; M_1 and W_α calculations have been made for three mean epoxy conversions, \bar{x} . Results are given in Table 2. The W_i values obtained are relatively consistent and in the

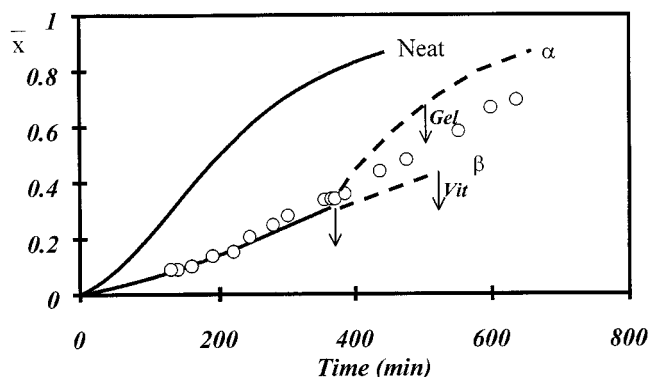


Figure 8. Kinetics of the epoxy–amine reaction in the blend with 48 wt % PEI at 135 °C: model taking into account only dilution effects for (—) one-phase and (---) two-phase domains and (○) experimental points (mean value, \bar{x} , after phase separation).

same range as the values obtained from TEM analysis (Figure 3).

From these results it is now possible to calculate the new dilution ratios in each phase as a function of reaction time for the 48 PEI system. Assuming that the stoichiometric ratio was not modified by the phase separation process, it is possible to predict the kinetics in α and β phases (Figure 8). To confirm this last hypothesis, an extraction of fully cured epoxy particles, postcured at 220 °C for 5 h, was performed by dissolving PEI. These particles exhibited a $T_g = 175.5$ °C close to the $T_{g\infty}$ of the final neat thermoset network, 177 °C (prepared at stoichiometry and without any additive).

Three different transformations—liquid–liquid phase transition (CP), gelation of the α phase, and vitrification of the β phase—are marked in Figure 8. The approximation seemed correct because the value of $x_{gel(\alpha)}$ found was in the range of 0.6. We expected that Figure 8 can provide a better understanding of the complex curing process and also point to the future experiments which are needed for a deeper description. For if someone needed to know if there are fractionation phenomena, modification of the stoichiometry ratio, preferential segregation of monomers,¹⁹ and low molar mass species in the β (or α) phase during the phase separation process, it would be necessary to have a complete knowledge of the phase compositions.

Conclusion

Rates of reaction in amorphous thermoplastic-modified epoxy systems were monitored using different techniques before and after phase separation. Depending on the initial concentration of thermoplastic, two behaviors were highlighted.

(i) For thermoplastic concentration ≤ 10 wt % no sudden change in the kinetic rates was detected when phase separation occurred, due to the low quantity of dispersed phase.

(ii) For thermoplastic concentrations higher than 30%, an increase of the reaction rate is observed when phase separation occurred, due to the appearance of a less

dilute epoxy–amine phase. A comparison between PS and PEI as thermoplastics showed a higher rate of reaction for PS blend after phase separation due to a lower viscosity of the blend during the first stages of the phase separation process. Microscopy and thermal measurements were used on a blend with 48 wt % PEI to make an estimation of the composition of each phase, leading to the predictions of the kinetic reaction rates in both phases. This prediction showed that gelation occurred for a conversion close to 0.6. These results helped us to understand the phenomenon occurring during the cure. However, there remains a need for a more direct technique to monitor the evolution of composition for each phase.

Acknowledgment. The contributions of H. Perier Camby (reactive extrusion) and I. Bornard (transmission electron microscopy) are gratefully acknowledged.

References and Notes

- (1) Williams, R. J. J.; Rozenberg, B. A.; Pascault, J. P. Reaction-induced phase separation in modified thermosetting polymers. *Adv. Polym. Sci.* **1996**, *128*, 95.
- (2) Girard-Reydet, E.; Sautereau, H.; Pascault, J. P.; Keates, P.; Navard, P.; Thollet, G.; Vigier, G. *Polymer* **1998**, *39*, 2269.
- (3) Pearson, R. A. In *Rubber Toughened Plastics I*; Riew, C. K., Kinloch, A. J., Eds.; *Adv. Chem. Ser.* **1993**, *233*, 407.
- (4) Vanderbosch, R. W.; Meijer, H. E. E.; Lemstra, P. J. *Polymer* **1995**, *36*, 2903.
- (5) Lemstra, P. J.; Kurja, J.; Meijer, H. E. E. In *Materials Science and Technology*; Cahn, R. W., Haasen, P., Kramer, E. J.; Eds.; Meijer, H. E. E., Ed.; Wiley VCH: Weinheim, 1997; Vol. 18, p 513.
- (6) Girard-Reydet, E.; Vicard, V.; Pascault, J. P.; Sautereau, H. *J. Appl. Polym. Sci.* **1997**, *65*, 2433.
- (7) Riccardi, C. C.; Borrajo, J.; Williams, R. J. J.; Girard-Reydet, E.; Sautereau, H.; Pascault, J. P. *J. Polym. Sci., Polym. Phys.* **1996**, *34*, 349.
- (8) Girard-Reydet, E.; Riccardi, C. C.; Sautereau, H.; Pascault, J. P. *Macromolecules* **1995**, *28*, 7599.
- (9) Horie, K.; Hiura, H.; Sawada, M.; Mita, I.; Kambe, H. *J. Polym. Sci.* **1970**, *8*, 1357.
- (10) Dusek, K.; Ilavsky, M.; Lunak, S. *J. Polym. Sci. Symp.* **1975**, *53*, 45.
- (11) Lunak, S.; Dusek, K. *J. Polym. Sci. Symp.* **1975**, *53*, 45.
- (12) Charlesworth, J. M. *J. Polym. Sci. Chem.* **1980**, *18*, 621.
- (13) Riccardi, C. C.; Adabbo, H. E.; Williams, R. J. J. *J. Appl. Polym. Sci.* **1984**, *29*, 2481.
- (14) Rozenberg, B. A. In *Epoxy Resins and Composites I*; Dusek, K., Ed.; *Adv. Polym. Sci.* **1995**, *72*, 113.
- (15) Verchère, D.; Sautereau, H.; Pascault, J. P.; Riccardi, C. C.; Moschiar, S. M.; Williams, R. J. J. *Macromolecules* **1990**, *23*, 725.
- (16) Min, B. G.; Hodgkin, J. H.; Stackurski, Z. H. *J. Appl. Polym. Sci.* **1993**, *50*, 1511.
- (17) Cao, Z. Q.; Méchin, F.; Pascault, J. P. *Polym. Int.* **1994**, *34*, 541.
- (18) Maazouz, A.; Becu, L.; Merle, G.; Taha, M. *J. Appl. Polym. Sci.*, in press.
- (19) Girard-Reydet, E.; Riccardi, C. C.; Sautereau, H.; Pascault, J. P. *Macromolecules* **1995**, *28*, 7608.
- (20) Swier, S.; Van Mele, B. Polymer Network Preprint P12, Trondheim, 1998.
- (21) Couchmann, P. R. *Macromolecules* **1978**, *11*, 1156.
- (22) Alig, I.; Jenninger, W. *J. Polym. Sci.* **1998**, *36*, 2461.
- (23) Bonnet, A.; Pascault, J. P.; Sautereau, H.; Camberlin, Y. *Macromolecules* **1999**, *32*, 8524.

MA981754P